Structural dependence on composition of rapidly quenched Fe-B alloys

F. H. Sánchez and M. B. Fernández van Raap
Departamento de Fisica, Facultad de Ciencias Exactas, Universidad Nacional de La Plata, Casilla de Correos 67, 1900 La Plata, Argentina

J. I. Budnick
Physics Department, University of Connecticut, 2152 Hillside Road, Storrs, Connecticut 06269
(Received 19 May 1992)

Based on the evolution of the rapidly quenched $Fe_{1-x}B_x$ alloy density, ^{57}Fe and ^{11}B hyperfine fields, ^{11}B NMR linewidth, and magnetic moment per alloy atom, in the composition range $0.01 \leq x \leq 0.25$, it is concluded that the short-range order around boron atoms in the amorphous alloys evolve from (orthorhombic) o-Fe_3B-like at $x \cong 0.12$ to (tetragonal) t-Fe_3B-like at $x \cong 0.22$–0.25. It is suggested that the microstructure of the amorphous alloys for x larger than but close to 0.12 resembles the fine dispersion of minute boride islands surrounded by iron observed in the crystalline system for $x \leq 0.09$, but with both boride and iron regions in amorphous states, in agreement with a model previously proposed by Dubois and Le Caer. The strong contribution of the interface boride/iron to the system free energy for alloys in the crystalline state is used to justify thermodynamically the crystalline to amorphous transition at $x \cong 0.12$ and again to crystalline at $x \cong 0.25$. Values are estimated for the free-energy formation of o-Fe_3B and of the interfaces o-Fe_3B/α-Fe and Fe_2B/α-Fe. Using a simple model for the formation of the boride particles in the rapidly quenched crystalline alloys, a relationship between particle radius and quenching rate is developed and from it a quenching rate–composition phase diagram is drawn, which reproduces qualitatively the main features of the iron-boron system.

INTRODUCTION

A better understanding of the iron-boron system should be helpful to understand other related systems, given the role that Fe-B interactions play in determining their structural and magnetic properties, especially anisotropy. Indeed, recognition of the importance of certain basic Fe-B structures in some new magnetic materials has begun to arise. It has been recently discovered that $Fe_{0.79}B_{0.17}Nd_{0.04}$ prepared in the amorphous state and subsequently crystallized becomes a hard magnet.[1] The boron environments in this material appear to be similar to those in the metastable phase tetragonal Fe_3B (t-Fe_3B).[2] It has been recently found[3] that there are two different boron environments in amorphous $Fe_{0.80}C_xB_{0.20-x}$. Two ^{11}B nuclear magnetic resonance frequencies were observed in this system, which agree with those reported for boron in t-Fe_3B and in its orthorhombic version (o-Fe_3B), respectively. Based on the different radio-frequency field amplitudes needed to excite ^{11}B in both sites, it was suggested that the o-Fe_3B-like environments are magnetically much softer than the t-Fe_3B-like ones. Thus, seemingly small differences in local order may lead to large differences in the physical properties, as the magnetic hardness in this case. Hopefully, the distinct magnetic properties of o-Fe_3B and t-Fe_3B could be used to the benefit of the design of new materials, taking advantage of the role that small additions of other elements (like the rare earths) play in improving their performances.[1]

Amorphous $Fe_{1-x}B_x$ alloys (hereafter a-$Fe_{1-x}B_x$) can be produced by rapidly cooling the melt to room temperature in a composition range from $x_1 \cong 0.12$ to $x_2 \cong 0.25$, though values of x_1 as low as 0.09 and of x_2 as high as 0.28 have been reported. For boron concentrations below x_1 the system crystallizes in a fine dispersion of o-Fe_3B in α-Fe. Above x_2 the alloys are again crystalline, basically a mixture of Fe_2B and α-Fe which may also contain other boride phases. The importance of Fe_3B in connection with the amorphous iron-boron structure has been pointed out. It is widely accepted that the t-Fe_3B structure is related to the short-range order of amorphous $Fe_{0.75}B_{0.25}$ and neighboring compositions ($0.20 \leq x \leq 0.25$). However, while some authors suggest that a SRO of the t-Fe_3B type also prevails in alloys with lower boron content,[4] some others have reported studies which give support for a connection between the o-Fe_3B structure and the amorphous local order[5,6] in the composition range $0.12 \leq x \leq 0.17$.

While it is clear that higher cooling rates are needed to produce the amorphous phase for compositions farther away from the eutectic ($x \cong 0.17$), and therefore to enhance the amorphous composition range, there is still little understanding of the meaning of *borders* x_1 and x_2 from a microscopic structural point of view. A possible question to be raised about this point is how are the microscopic structures below and above x_1 related, and whether this relationship plays an active role in determining this composition.

As mentioned above, another fundamental question concerns the short-range order at the metal and metalloid sites in the amorphous alloys. The knowledge of the local order is important for the understanding of the properties of the amorphous system and their correlation with those

of the crystalline intermetallics. Access to this knowledge is difficult, however, due to the main characteristic of the amorphous state, namely, the lack of long-range order. This feature limits the power of conventional structural techniques, such as x-ray diffraction (XRD). Even so, the combined application of XRD and neutron diffraction has given crucial information concerning the average number of Fe-Fe, Fe-B, and B-B near-neighbor pairs and their respective mean separation, as well as on the average atomic magnetic moments.[7,8] In some cases, the simultaneous application of local probe techniques, such as the Mössbauer effect (ME) and nuclear magnetic resonance (NMR) has contributed to a more refined description of the atomic ordering in the immediate surroundings 2–4 Å) of both constituents.[9] But even these local techniques are in general of limited value due to the fact that the signals originate in a quasicontinuous distribution of sites, which produces a broad distribution of the signals themselves. This is aggravated in the case of NMR and especially ME spectra, where distributions of both hyperfine magnetic interactions and of electric quadrupole interactions (including the isomer shifts) are correlated in a generally unknown manner. The spectral analyses are also often complicated due to large effective thickness, spin texture, and magnetic anisotropy.

A recently initiated alternative[10–13] is the study of metastable crystalline alloys prepared by identical means but with boron concentrations below the *composition border* for amorphous formation. In these systems, as in the amorphous alloys, the coordination shell of a boron atom is exclusively composed of iron atoms. There are good reasons to assume that it is the metalloid-metal interaction which determines the short-range order. The purpose of these studies has been therefore to investigate the type of local order that the metalloid atoms induce in their neighborhood under the conditions of fast cooling which exist in the melt spinning process, while at the same time avoiding the complexity of the amorphous signals. The ultimate objective was to determine a possible connection between the local structures in the alloys prepared in both states.

Here, we discuss the outcome of these studies along with some newer results[14,15] generated from alloys more concentrated in boron, although still below the *border* x_1 for amorphous formation. From this analysis we propose a description of $Fe_{1-x}B_x$ rapidly quenched alloys in a wide composition range ($0 \le x \le 0.25$). As we shall discuss below, this picture is based on the existence of three composition regions, $0 \le x \le x_0$, $x_0 \le x \le x_1$, and $x_1 \le x \le x_2$ (where x_0, x_1, and x_2 are about 0.09, 0.12, and 0.25, respectively), with different local order and with a different degree of order. o-Fe_3B plays an important part in this picture. Our description will be discussed in connection to models previously proposed by Gaskell,[16] Hamada and Fujita,[17] and Dubois and Le Caer[18] for the range $x_1 \le x \le x_2$ in order to offer a more consistent view of the Fe-B rapidly quenched system. A tentative explanation of the meaning of the *composition borders* x_1 and x_2 for amorphous formation will be given, based on thermodynamic and kinetic considerations.

THE MICROSTRUCTURE OF THE $Fe_{1-x}B_x$ SYSTEM PREPARED BY MELT SPINNING FOR COMPOSITIONS BELOW BORDER x_1

By adjusting properly the cooling rate parameters, seemingly uniform crystalline alloys (c-$Fe_{1-x}B_x$) can be produced in the range $0.01 \le x \le 0.12$ (this same cooling rate would produce amorphous alloys for larger values of x). Although XRD, desitometry and magnetization measurements carried out on these alloys could be explained assuming a special type of substitutional solid solution of boron into bcc iron,[19] experiments probing the system more locally, like ME and NMR, have shown that these alloys are indeed heterogeneous.[10,11] In the range $0.01 \le x \le 0.09$, it has been proven that the system consists of a fine dispersion of minute o-Fe_3B-like particles or complexes, embedded in a bcc-Fe matrix which becomes more and more disordered as x increases [see Fig. 1(a)]. Support for this description has come from high-resolution transmission electron microscopy and selected area electron diffraction experiments,[12] which revealed that the boride complexes have sizes from 5 to 15 Å. The system has been found surprisingly stable,[13] taking into account that o-Fe_3B is itself a very unstable phase and that the boride particles are so small. The observed stability indicates that the energy at the interface particle/matrix is low which in turn would result from a good matching of the microstructures at both sides of the interface. This is in fact visible in high-resolution TEM studies,[12] and is further confirmed by the absence of Mössbauer and NMR signals which could be associated with probes in border transition regions between the boride cores and the bcc-Fe matrix.[10,11]

For higher boron concentrations, namely, $x \cong 0.11$, 0.12, the system becomes more complex. As it had been already observed in samples with less boron ($x \le 0.09$),[10] the ME spectra indicate that the majority of the ^{57}Fe

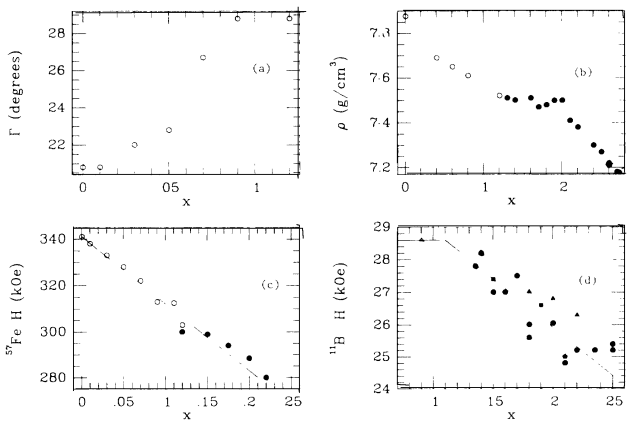

FIG. 1. (a) α-Fe (110) x-ray diffraction line full width (Ref. 12), (b) alloy density (Refs. 19 and 20), (c) ^{57}Fe hyperfine field (Refs. 10, 15, and 18), and (d) ^{11}B hyperfine field (Refs. 5, 6, 11, and 21–23), for $Fe_{1-x}B_x$ rapidly quenched alloys as a function of composition. Open circles correspond to crystalline alloys while other symbols represent values obtained from the amorphous state.

probes are in bcc, α-Fe-like, environments, but there are at least four other Fe sites which have been associated with the boride(s) phase(s).[15] Their populations and hyperfine interactions (magnetic hyperfine fields H of approximately 288, 270, 249, and 235 KOe) do not match with any single known boride phase, nor with a mixture of them. The fact that the hyperfine fields at these four sites show the same temperature dependence strongly suggests that they correspond to a single phase. Based on the relative intensities of the Mössbauer signals, it has been concluded that this boride phase has a Fe/B atomic ratio of about three.[15] In two of the boride sites ($H \cong 235$, 270 kOe) the ^{57}Fe probes experience interactions similar to those observed in o-Fe_3B. These sites are significantly populated. Furthermore, in a rather low temperature step (673 K $\leq T \leq$ 716 K), the part of the Mössbauer spectra associated with the boride becomes more similar to that of o-Fe_3B, with no clear evidence for metallic iron segregation. By a consideration of the correlation between the ^{57}Fe hyperfine field and the number of boron near neighbors (n_{FeB}) to the ^{57}Fe probe site,[18] it was found that, on the average, $n_{FeB} \cong 3$ and $n_{BFe} = n_{FeB} f_B (1-x)/x \cong 9$ as in both types of Fe_3B (where f_B is the fraction of ^{57}Fe probes in the boride and n_{BFe} stands for the number of Fe near neighbors to a B atom). All these facts suggest that the original boride phase may be a sort of modified and disordered o-Fe_3B. The only sign that XRD measurements give for the boride phase (which according to the ME results contains about 37% of the Fe atoms) is a distribution of diffracted radiation of low intensity located in a narrow angular range immediately before the most intense bcc α-Fe reflection. The ME linewidths are considerably wide in this composition range, to the extent that the description of the boride signal by means of a distribution of magnetic interactions of the type observed in the amorphous alloys cannot be completely ruled out. To some extent, these considerations give support to studies[5,6] which suggested a local order of o-Fe_3B type for amorphous $Fe_{0.86}B_{0.14}$.

EVOLUTION OF DENSITY, HYPERFINE FIELDS, AND MAGNETIC MOMENTS ($0 \leq x \leq 0.25$)

Next we shall comment on the behavior of the alloy density, mean atomic magnetic moment, and average hyperfine fields at Fe and B locations in the range $0 \leq x \leq 0.25$, and especially across the *amorphization border* x_1. The alloy density is shown in Fig. 1(b) where results obtained by Hasegawa, Ray, and co-workers from the crystalline[19] and from the glassy[20] state are displayed together. The continuity of the density (and its slope) at $x_1 \cong 0.12$ is remarkable, suggesting that the microstructures below and above x_1 have something in common. A similar conclusion can be drawn from the dependence of the average ^{57}Fe hyperfine field, H_{Fe}, with composition. H_{Fe} obtained at 4.2 K from crystalline[10,15] and from amorphous[18] alloys is shown in Fig. 1(c), which indicates an almost linear dependence of this quantity with x, with no gap at $x = x_1$. The ^{11}B mean hyperfine field H_B at 4.2 K is displayed in Fig. 1(d) as a function of x. H_B does not vary for $x \leq 0.09$, as the boride phase does not change in this composition range,[10,11] but it decreases in a seemingly linear manner for $0.135 \leq x \leq 0.22$.[5,6,21-24] The extrapolation of the two tendencies intersects somewhere in the vicinity of $x = 0.12$. The decreasing of H_B suggests a variation of the boron SRO toward a t-Fe_3B-like local structure which appears to be achieved at or above $x = 0.22$, given the similarity of the ^{11}B hyperfine fields in the amorphous and in t-Fe_3B (25.2 kOe). Support for this conclusion comes also from the ^{57}Fe mean hyperfine field which, for $x \cong 0.25$ has approximately the same value as in t-Fe_3B (275 kOe). It is also interesting to consider the variation of the ^{11}B NMR linewidth with composition. In Fig. 2(a) the resonance width is shown for alloys prepared by the group of Hasegawa at Allied Corporation, and measured by Zhang *et al.*[11,25] and by Ford *et al.*[23]. The plot indicates that the disorder in the boron surroundings increases with increasing boron concentration, and again the result from the metastable crystalline system ($x = 0.09$) matches consistently with the trend set by the results from the amorphous samples.

Finally, the composition dependence of the magnetic moment per alloy atom at 4.2 K is represented in Fig. 2(b). Results obtained from measured ^{57}Fe hyperfine fields[10,15] using the empirical relation $\mu_{Fe} \cong (H_{Fe}/130)\mu_B/\text{kOe}$, properly weighted with the relative site abundances and renormalized per alloy atom, have been included along with the results from magnetization experiments.[19,26] The continuity of $\mu(x)$ and its derivative $(\partial\mu/\partial x)(x)$ across $x_1 \cong 0.12$ is apparent, as happened with most of the physical quantities discussed above.

As we have pointed out above, all these results suggest that the microstructures of c-$Fe_{1-x}B_x$ and a-$Fe_{1-x}B_x$ alloys at both sides of the *amorphization border* x_1 have something in common. One is tempted to imagine that the picture of minute boride islands embedded in iron remains valid for $x \geq x_1$, with the important difference that both phases are now *amorphous* instead of *crystalline*. This image agrees with the model proposed by Dubois and LeCaer[18] for a-$Fe_{1-x}B_x$ in the range $x_1 \leq x \leq x_s$ where $x_s \cong 0.155$, which is based on a study of the density

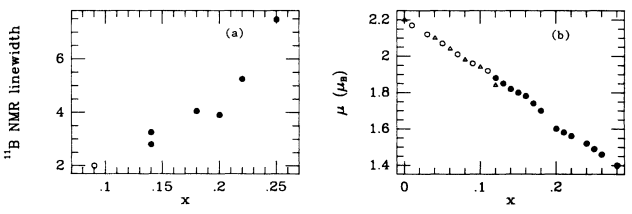

FIG. 2. (a) ^{11}B NMR linewidth (Refs. 5, 11, and 23) and (b) magnetic moment per alloy atom (Refs. 10, 15, 19, and 26), for $Fe_{1-x}B_x$ rapidly quenched alloys as a function of composition. Open symbols correspond to crystalline alloys while solid symbols represent results obtained from the amorphous state. In (b) the triangles correspond to values estimated from Mössbauer ^{57}Fe hyperfine fields.

and of the ^{57}Fe hyperfine fields for alloys in the amorphous state. Actually, the size of the amorphous boride islands suggested by them ($\cong 15$ Å) is consistent with the size of the complexes observed by us in the crystalline state.[12] Following Dubois and Le Caer's description, this situation would reverse (amorphous iron islands in an amorphous boride matrix) when $x_s \leq x \leq x_c$ ($x_c \cong 0.20$), and finally the alloys would become homogeneous for $x_c \leq x \leq x_2$.

Within the frame of this model the enlargement of the ^{11}B NMR linewidth with x can be interpreted in the following way. Due to the lower directionality of the Fe-Fe bonds (as compared to the B-Fe bonds), the iron regions would work as a sort of *hinges* or *stress dissipators* which would allow the local order around the boron atoms to be preserved locally, while the long-range order is lost. As x increases the effect of the softer iron regions (which become thinner and smaller in number) reduces and finally becomes null for $x \cong 0.25$. Hence, in order to obtain $a\text{Fe}_{0.75}B_{0.25}$ (i.e., in order to destroy the positional and orientational long-range order) the disorder around the boron atoms has to be larger. This interplay between the Fe-Fe and B-Fe bonds has been detected before[9] by means of a combined NMR and Mössbauer study of the primary crystallization of a-$\text{Fe}_{0.86}\text{B}_{0.14}$. It was observed that, at an intermediate crystallization state, the ^{57}Fe Mössbauer signals from the amorphous phase remained *amorphouslike* while an important fraction of the ^{11}B NMR signal (from the same phase) became *crystalline-(t-*Fe_3B*)-like.* This result was interpreted on the basis of the existence of local disorder around the iron probes but local order around the boron ones.

In their model, Dubois and Le Caer assume that the amorphous boride regions have a t-Fe_3B SRO in the whole composition range. The results presented in this section suggest that near the lower *concentration limit* x_1 the SRO around the boron atoms would probably be more similar to that of o-Fe_3B.

ON THE SEGREGATION OF THE o-Fe_3B COMPLEXES FROM AN α-$\text{Fe}_{1-x}\text{B}_x$ bcc SOLID SOLUTION DURING THE MELT-SPINNING PROCESS

As we have mentioned before the solubility of boron in iron is very small. However, boron is slightly more soluble in γ(fcc)-Fe than in α(bcc)-Fe[27]. We may then suppose that the boride segregates during the fast cooling process essentially after the system becomes bcc structured, either through an undercooled liquid$\rightarrow$bcc or through a fcc$\rightarrow$bcc transformation. Under the kinetic conditions prevailing during the melt-spinning process, the formation of the bcc phase may occur at temperatures considerably lower than the equilibrium transformation temperature. Since diffusion is a process strongly dependent on temperature (for instance, for a diffusion energy $E_D \cong 2$ eV/at, $D(T_2=800\ \text{K})/D(T_1=900\ \text{K}) \cong .04$) we will just consider segregation of the boride while the system undergoes the first 100 K of cooling in the bcc phase. We shall assume that nucleation of o-Fe_3B occurs homogeneously and isotropically.

We shall consider a spherical region of the α-$\text{Fe}_{1-x}\text{B}_x$ solid solution of radius R_0 from which a single o-Fe_3B spherical particle of radius r_p is formed. Let η_p and η_0 be the number of atoms in the boride particle and in the original region of the solution, and V_p and V_0 the respective volumes. In terms of η_0 and η_p the ratio of volume V_p to V_0 is given by

$$V_p/V_0=(r_p/R_0)^3=(\eta_p v_B)/(\eta_0 v_\alpha) , \tag{1}$$

where v_B and v_α represent the volumes per atom of o-Fe_3B and α-$\text{Fe}_{1-x}\text{B}_x$.

Now, we shall estimate the mean distance $\bar{R}$ that the boron atoms must diffuse to form a boride particle in the center of the volume V_0. Calling $r(R)$ the radius of the particle which wold be formed with the material contained inside a sphere of solution of radius R ($0 \leq R \leq R_0$),

$$\bar{R} \cong (1/V_0)\int_0^{R_0} 4\pi R^2[R - r(R)]dR . \tag{2}$$

Now, $r(R)/R = r_p/R_0$, so using (1) Eq. (2) becomes

$$\bar{R} \cong 3R_0[1-(\eta_p v_B/\eta_0 v_\alpha)^{1/3}]/4 , \tag{3}$$

or, in terms of r_p,

$$\bar{R} \cong 3r_p[(\eta_0 v_\alpha/\eta_p v_B)^{1/3}-1]/4 . \tag{4}$$

$\bar{R}$ is related to the diffusion constant D and diffusion time t through $\lambda(Dt)^{1/2}=\bar{R}$, where λ is a constant of the order of unity (here we shall set $\lambda=1$). Furthermore, the diffusion time t can be estimated from the temperature interval ΔT where segregation takes place and from the quenching rate Q_R, through $t \cong \Delta T/Q_R$. Therefore, (4) can be written in the form

$$D \cong \{3r_p[(\eta_0 v_\alpha/\eta_p v_B)^{1/3}-1]/4\}^2 Q_R/\Delta T , \tag{5}$$

where $\eta_p/\eta_0 = 4x$, and $v_B \cong 10$ Å^3/atom. Furthermore, assuming that α-$\text{Fe}_{1-x}\text{B}_x$ is an interstitial solution, $v_\alpha \cong 11.8(1-x)$ Å^3/atom.

AMORPHIZATION RANGE

Based on the evolution of the microstructure of the Fe-B rapidly quenched system with composition we shall estimate the contributions to the system free energy and discuss the occurrence of the amorphous phase for $0.12 \leq x \leq 0.25$ in connection with the available thermodynamic data. In order to simplify our task we will distinguish only three composition regions.

(i) $x \leq x_1$. Under the kinetic conditions of the *melt-spinning* process, and given the extremely low solubility of boron into iron,[27] the microstructure characterized by minute boride islands disperse in the bcc-Fe matrix is formed. This state of high dispersion maximizes the interface contribution to the free energy of the mixture, $G_M(x)$,

$$G_M(x)=N_\alpha(x)\cdot G_\alpha + N_B(x)\cdot G_B + N_S(x)\cdot\sigma . \tag{6}$$

Here $N_\alpha(x)$, $N_B(x)$, and $N_S(x)$ are the numbers of gram atoms in α-Fe, o-Fe_3B, and at the interface, and G_α, G_B,

and σ are the respective free energies per gram atom at room temperature.

(ii) $x_1 \leq x \leq x_2$. Amorphous alloys are produced. If they were homogeneous it would be no interface. If the amorphous system is inhomogeneous, with ironlike and boridelike regions, we shall assume that atoms at the interface are free enough as to find positions which minimize the interface free-energy contribution to $G_{am}(x)$ to the extent that it can be neglected.

(iii) $x > x_2$. Again crystalline heterogeneous systems, α-Fe+Fe_2B (which may also contain other borides), are formed. The free energy shall be estimated using (6), where $N_B(x)$ and G_B now represent the number of gram atoms of Fe_2B and its free energy per gram atom.

For the microstructures proposed for regions (i) and (iii), the interface area $a(x)$ will have a maximum for a composition intermediate between $x=0$ (pure iron) and $x=x_m$ (pure boride; $x_m=0.25$ for Fe_3B, $x_m=0.33$ for Fe_2B). We approximate $a(x)$ with the simplest function having a single maximum at $x=x_m/2$,

$$N_S(x)=\nu\cdot a(x)\cong\nu\cdot K\cdot(x_m-x)\cdot x \ , \tag{7}$$

where ν is the number of gram atoms per area unit at the interface. In Eq. (7), K is a constant that can be determined taking into account that for $x \ll x_m$, $a(x)$ increases linearly with the number of boride particles, $N_p(x)$, and is proportional to the mean particle area, a_p,

$$a(x)\cong N_p(x)\cdot a_p, \quad x \ll x_m \ ,$$

which leads to

$$K=3/(n_B\cdot r_p\cdot x_m^2) \ , \tag{8}$$

where r_p is the mean radius of the boride complexes and n_B is the number density of the boride.

For certain critical composition value, the additional interface contribution present in the crystalline mixture, $N_S(x)\cdot\sigma$, may bring the system free energy beyond that corresponding to the amorphous state, where this contribution is either absent or can be neglected. This term should be of special relevance when the system is finely divided, as in our case, and would become important in determining the *amorphous border* x_1. We shall inquire which values of the free energy interface densities of α-Fe/o-Fe_3B and α-Fe/Fe_2B, and of the free energy volume density G_B of o-Fe_3B, are compatible with the known microstructure of the $Fe_{1-x}B_x$ alloys, and we shall test the consistency of these estimated values against experimental studies of the thermally induced transformation of the α-Fe/o-Fe_3B dispersion into an α-Fe/Fe_2B mixture.[13]

In order to go further we will assume that the o-Fe_3B complexes segregate from a solid solution α-$Fe_{1-x}B_{x'}$ [α-Fe(B)], during the fast cooling process. Then, from elemental nucleation theory we can write

$$\sigma=\Delta G(x')\cdot n_B\cdot r_c(x')/2\nu \ , \tag{9}$$

where $r_c(x')$ is the o-Fe_3B nuclei critical radius and $\Delta G(x')$ is given by

$$\Delta G(x') = G_{\alpha\text{-Fe(B)}}(x')-[N_\alpha(x')\cdot G_\alpha+N_B(x')\cdot G_B] \ . \tag{10}$$

Substituting (10) into (9) and in turn (9) into (6), we get an equation from which expressions for G_B and σ can be obtained:

$$G_B=\frac{G_M(x)-3x(x_m-x)r_c(x')G_{\alpha\text{-Fe(B)}}(x')/2r_p x_m^2}{x/x_m-3x(x_m-x)r_c(x')x'/2r_p x_m^3} \ , \tag{11}$$

$$\sigma=[G_{\alpha\text{-Fe(B)}}(x')-x'G_B/x_m]n_B r_c(x')/2\nu \ , \tag{12}$$

where we have used $N_\alpha(x)=1-x/x_m$ and $N_B(x)=x/x_m$. In expressions (11) and (12) we have chosen the free energy for α-Fe as the free energy zero ($G_\alpha=0$). The critical radius $r_c(x')$, will be approximated by the minimum observed complex radius $r_p^{\min}\cong 5$ Å (which has not been detected to depend on composition[12]). In Eq. (11) we have kept artificially the distinction between x and x' (the last one introduced in the calculation of σ) because we shall make the additional assumption that σ is composition independent [under the present conditions this is equivalent to assume a linear composition dependence for $G_{\alpha\text{-Fe(B)}}(x')$]. This assumption shall allow us to use numerical values of $G_{\alpha\text{-Fe(B)}}(x')$ reported for a limited composition range.[28]

Finally, from the fact that the $Fe_{1-x}B_x$ alloys form in the amorphous state for $x \geq x_1 \cong 0.12$, we shall set $G_M(0.12)\cong G_{am}(0.12)$. Taking $G_{am}(x)$ from Ref. 28 we get

$$\begin{aligned} &G_B\cong -4 \text{ kJ/g atom} \quad (o\text{-}Fe_3B) \ , \\ &\sigma\cong 4.5 \text{ kJ/g atom} \quad (\alpha\text{-Fe}/o\text{-}Fe_3B) \ , \end{aligned} \tag{13}$$

where we have used $\nu\cong 0.3$ atom/Å^2.

By a similar procedure, now for the upper *amorphization border* x_2, and using values for $G_B(Fe_2B)$ and $G_{am}(x)$ from Ref. 28 we obtain

$$\sigma\cong 50 \text{ kJ/g atom} \quad (\alpha\text{-Fe}/Fe_2B) \ . \tag{14}$$

The curves in Fig. 3 have been constructed from Eq. (6) using results (13) and (14) and the results reported by Clavaguera-Mora *et al.*[28] for Fe_2B and a-$Fe_{1-x}B_x$. These curves indicate that, starting from the amorphization range experimentally observed, the absence of Fe_2B in the rapidly quenched alloys for $x \leq x_1$ and the preeminence of this compound for $x \geq x_2$, become justified. Results (13) and (14) are also consistent with the observation[13] that in c-$Fe_{0.91}B_{0.09}$ the transformation o-$Fe_3B \rightarrow Fe_2B$ would involve many o-Fe_3B complexes to produce a single Fe_2B particle, since the transformation of a single particle ($\cong 15$ Å) should be energetically unfavorable due to the strong increase in the interface energy. It may prove interesting to perform computer calculations of the free formation energies G_B (o-Fe_3B) and σ (o-Fe_3B/α-Fe and Fe_2B/α-Fe interfaces) and compare the results with the values given in (13) and (14).

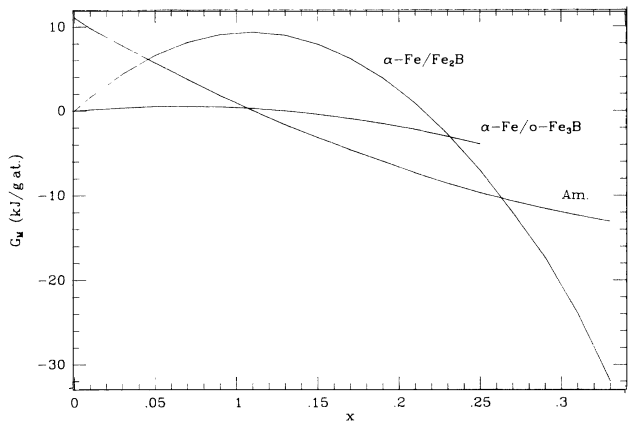

FIG. 3. Free energy curves calculated for fine dispersions of α-Fe and Fe_2B, and of α-Fe and o-Fe_3B, using Eqs. (6)–(8), (13), and (14) (see text). The free energy curve for amorphous $Fe_{1-x}B_x$ (Ref. 28) is also shown. It can be seen that the minimum free energy between $x \cong 0.11$ and $x \cong 0.26$ correspond to the amorphous state.

Now, the amorphization range (x_1, x_2) can be estimated as a function of the quenching rate Q_R. To do this we derive first the dependence of r_p on Q_R from (5) and then we obtain $G_M(x)$, from (6), for mixtures of α-Fe and o-Fe_3B, and of α-Fe and Fe_2B, in terms of Q_R. Then, we compare these $G_M(x)$ values with each other as well as with the $G_{\alpha m}(x)$ values reported in Ref. 28. From this comparison we get a partial phase diagram of the Fe-B system in terms of x and Q_R for the four phases α-Fe, o-Fe_3B, Fe_2B, and a-$Fe_{1-x}B_x$ alloys, which is shown in Fig. 4. In this process, the condition $r_p = 5$ Å for $Q_R = 10^7$ K/s has been imposed. Although it is difficult to estimate the magnitude of the errors involved in the preceding calculations, it becomes clear to us that there must be large uncertainties in the phase diagram of Fig. 4, especially in connection with the quenching rate value. Even

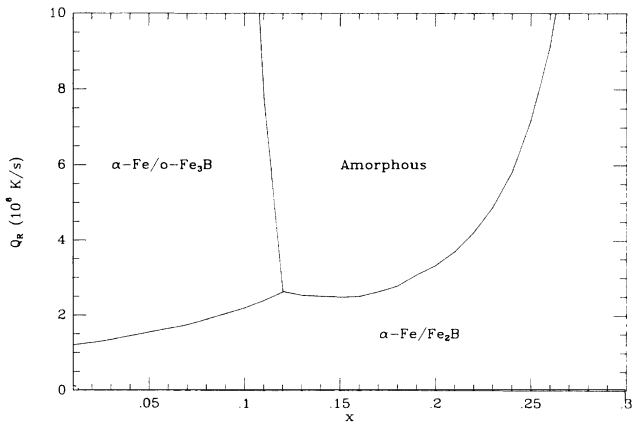

FIG. 4. Quenching rate vs composition partial phase diagram for α-Fe, o-Fe_3B, Fe_2B, and amorphous alloys. The diagram reproduces qualitatively the main features of the iron-boron system.

so, it is worth noticing that it reproduces qualitatively the main features observed in rapidly quenched Fe-B alloys as, for instance, the difficulty for preparing amorphous alloys for compositions far below $x \cong 0.12$ or far above 0.25, and the enhancement of the range (x_1, x_2) as Q_R increases. Figure 4 also shows the composition region where formation of Fe_2B instead of o-Fe_3B should be expected. For instance, for $Q_R \cong 1.5 \times 10^6$ K/s, Fe_2B would form for $x \geq 0.05$. Finally, it must be noticed that the existence of the deep eutectic around $x \cong 0.17$ has not been taken into account in the precedent analysis.

DISCUSSION AND CONCLUSIONS

One of the main conclusions of the present study comes from the similar values of density and several atomic averaged quantities such as ^{57}Fe and ^{11}B hyperfine fields, ^{11}B NMR linewidth, atomic magnetic moment, at both sides of the *amorphization border* x_1. This conclusion is that it must be a correspondence between the local structures of the crystalline and amorphous states for $x \cong x_1$. Since it has been demonstrated that for $x \leq x_1$ the boride phase is highly disperse in the iron matrix, we suggest that for x larger but close to x_1 the amorphous microstructure imitates this fine dispersion. From the identification (for $x \leq x_1$) of the boride as o-Fe_3B (Refs. 10 and 11) or a modified form of this compound,[15] we conclude that in the vicinity of composition x_1 the amorphous boride zones have a SRO which resembles that of o-Fe_3B. This picture differs from several others which describe the amorphous phase as homogeneous. While some authors[4] have proposed a t-Fe_3B-like SRO, with iron gradually substituting the boron atoms as x decreases toward x_1, others[26] have suggested a bcc-like SRO for x near x_1. Evidences for an o-Fe_3B-like SRO[5,6] have been also presented for $x \cong x_1$.

Descriptions of the a-$Fe_{1-x}B_x$ alloys as inhomogeneous at a nanoscopic scale have been proposed before. Hamada and Fujita[17] proposed a model in which bcc-like crystalline embryos are surrounded by disordered regions. In addition they introduced chemical clusters of Fe_3B for alloys with larger boron content. By keeping the size of embryos and clusters below 10 Å they were able to calculate interference and pair-correlation functions which are in good agreement with the experiments.

Gaskell[16] has constructed a model based on the local coordination polyhedra found in crystalline systems, and actually imitating the edge-sharing arrangement found in o-Fe_3C (isostructural with o-Fe_3B). For $x = 0.2$ a representation of this model is a collection of branched polymeric chains of mTM_6 trigonal prism units (m = metalloid, TM = transition metal). When this model is extended to lower values of x, the polymeric chains have to be shortened or the prisms have to share corners instead of edges. In any case the extreme situation will correspond to chains one unit long, i.e., not polymerization at all. Even in this case the composition will be $x = 0.143$, and any attempt to simulate amorphous with even lower x values will have to assume pure iron regions besides the trigonal prism chains. Furthermore, if as suggested by

Gaskell, polymerization contributes to the stabilization of the system, the additional iron regions would be needed at higher boron concentrations. For instance, assuming arbitrarily that at least five mTM_6 units per chain are needed to guarantee stability, the iron regions should coexist along with the chains for x below 0.185.

Finally, Dubois and Le Caer,[18] based on Mössbauer studies concluded that there are two kinds of iron environments in hypoeutectic amorphous Fe-B alloys. They suggested that part of the iron atoms are embedded in capped trigonal prisms (forming boride A_B regions), and that the rest have no boron neighbors and fill the space between the boride regions (A_{Fe} regions). For $x \leq x_s \cong 0.15-0.16$ they propose a picture where A_B islands are surrounded by a continuous A_{Fe} "phase." For x between x_s and $x_c \cong 0.20$, the description is reversed with the A_{Fe} zones enclosed by the A_B boride. Above x_c the amorphous would be homogeneous, A_B type. In the A_B regions the iron atoms are assumed to have two to three boron neighbors, and the boron atoms about nine iron neighbors, as in Fe_3B. Based on the change of the density slope at $x \cong 0.2$ [see Fig. 1(b)], these authors suggested that the stacking of iron in the A_{Fe} zones may resemble that of bcc-iron.

The common feature of these three models with ours is that they consider the coexistence of Fe-like and Fe_3B-like regions to describe iron-rich a-$Fe_{1-x}B_x$ alloys. In the models of Hamada and Fujita[17] and Dubois and Le Caer,[18] this assumption is introduced in order to give account of Mössbauer and diffraction experiments. The size of the boride and/or iron complexes proposed by them coincides with the dimension of the o-Fe_3B complexes observed by us[12] for $x \leq 0.09$. In the model of Gaskell (for amorphous of compositions mTM_4 and mTM_5 the iron clusters have to be included in order to extend the description to lower metalloid concentrations. On the other hand our model is based on the structure of the metastable crystalline alloys for $x \leq x_1$, as well as on the continuity of the alloy density and hyperfine interaction parameters at the *composition border* x_1 for amorphous formation. In general terms our description agrees better with that of Dubois and Le Caer.[18]

From the thermodynamic point of view we have brought the free energy due to the formation of the interface boride/iron into consideration. In a system so finely divided as the rapidly quenched c-$Fe_{1-x}B_x$ alloys ($x \leq x_1$) this contribution may become very important. In this sense compounds with higher formation energies may form if this increase in the free energy is compensated by the reduction of the interface contribution. Therefore the formation of o-Fe_3B instead of the more stable t-Fe_3B or Fe_2B becomes favorable for $x \leq x_1$, and when the interface area increases beyond a certain limit ($x \cong x_1$) the formation of amorphous alloys occurs because it would require even less free energy than the formation of the dispersion of o-Fe_3B in α-Fe. This situation is driven by the kinetic conditions present during the system formation. Under lower cooling rate conditions, long-range diffusion would take place and large precipitates of the stable compound Fe_2B would be formed. This has been represented in Fig. 4, where the competition expected among the formation of $Fe_2B+\alpha$-Fe, o-$Fe_3B+\alpha$-Fe, and a-$Fe_{1-x}B_x$ for different quenching rates is shown.

In a certain way it is surprising that the interface contribution is not taken into account more often in regard to nano structures. For instance, it may be interesting to study the influence of this contribution during the solid-state reaction-induced amorphization (SSRA) processes.[29] In these processes the reacting elements have to be brought into a state of fine and intimate mixture before the reaction is started. By this means, only short-range diffusion (of the order of the original particles size or layer thickness) is needed in order to mix the constituents, which is achieved by moderate temperature treatments. Under these circumstances, crystalline compounds would be normally produced in the form of incoherent nanocrystals giving rise to a large interface (or grain border) area, and the interface contribution to the system free energy would be again magnified. Therefore, formation of amorphous phases with the elimination of this contribution may become energetically favorable.

ACKNOWLEDGMENTS

We wish to acknowledge L. A. Mendoza Zélis, Y. D. Zhang, and W. A. Hines for many useful discussions. This work was supported in part by the Consejo Nacional de Investigaciones Cientificas y Tecnologicas (CONICET), of the República Argentina.

[1]K. H. J. Buschow, in *Supermagnets, Hard Magnetic Materials*, NATO ASI Series Vol. 331, edited by G. J. Long and F. Grandjean (Kluwer Academic in cooperation with NATO Scientific Affairs Divison, Boston, 1991), p. 29.16.

[2]Y. Zhang, J. I. Budnick, J. C. Ford, and W. A. Hines (unpublished).

[3]S. H. Ge, M. X. Mao, G. L. Chen, C. L. Zhang, Y. D. Zhang, W. A. Hines, and J. I. Budnick (unpublished).

[4]I. Vincze, T. Kemny, and S. Arajs, Phys. Rev. B **21**, 937 (1980).

[5]Y. Zhang, J. I. Budnick, Ford, W. Hines, F. H. Sánchez, and R. Hasegawa, J. Appl. Phys. **61**, 3231 (1987).

[6]V. S. Pokatilov, Dok. Akad. Nauk SSSR **275**, 79 (1984) [Sov. Phys. Dokl. **29**, 234 (1984)].

[7]P. Lamparter, E. Nold, G. Rainer-Harbach, E. Grallath, and S. Steeb, Z. Naturforsch. **36a**, 165 (1981); P. Lamparter, W. Sperl, S. Steeb, and J. Blétry, *ibid.* **37**a 1223 (1982); E. Nold, P. Lamparter, H. Olbrich, A. Rainer-Harbach, and S. Steeb, *ibid.* **36a**, 1032 (1981).

[8]Y. Waseda and H. S. Chen, Phys. Status Solidi A **49**, 387 (1978); T. Fujiwara, H. S. Chen, and Y. Waseda, J. Phys. F **11**, 1327 (1981).

[9]F. H. Sánchez, Y. Zhang, and J. I. Budnick, Phys. Rev. B **38**, 8508 (1988).

[10]F. H. Sánchez, J. I. Budnick, Y. Zhang, W. Hines, M. Choi, and R. Hasegawa, Phys. Rev. B **34**, 4738 (1986).

[11]Y. Zhang, W. Hines, J. I. Budnick, M. Choi, F. H. Sánchez,

and R. Hasegawa, J. Magn. Magn. Mater. **61**, 162 (1986).
[12]J. I. Budnick, F. H. Sánchez, Y. Zhang, M. Choi, W. Hines, Z. Zhang, Ge, and R. Hasegawa, IEEE Trans. Mag. **23**, 1937 (1987).
[13]M. B. Fernández van Raap and F. H. Sánchez, J. Appl. Phys. **66**, 875 (1989).
[14]M. B. Fernández van Raap and F. H. Sánchez, in *Applications of the Mossbauer Effect,* Proceedings of the First Latin American Conference, edited by E. Baggio-Saitovich, E. Galvao da Silva and Y. H. R. Rechenberg (World Scientific, Singapore, 1990), p. 278.
[15]M. B. Fernández van Raap and F. H. Sánchez (unpublished).
[16]P. H. Gaskell, J. Non-Cryst. Solids **32**, 207 (1979).
[17]T. Hamada and F. E. Fujita, Jpn. J. Appl. Phys. **24**, 249 (1985).
[18]J. M. Dubois and G. Le Caer, Nucl. Instrum. Methods **199**, 307 (1982).
[19]R. Ray and R. Hasegawa, Solid State Commun. **27**, 471 (1978).
[20]R. Ray, R. Hasegawa, C.-P. Chou, and L. A. Davis, Scr. Metall. **11**, 973 (1977).
[21]V. S. Pokatilov, Dok. Akad. Nauk SSSR **257**, 95 (1981) [Sov. Phys. Dokl. **26**, 327 (1981)].
[22]G. Le Caer, B. Lemius, J. Welfringer, E. Bauer-Grosse, and J. M. Dubois, in *Amorphous Metals and Non-Equilibrium Processing,* edited by M. von Allmen (Les Editions de Physique, Strasbourg, 1984), p. 265.
[23]J. C. Ford, J. I. Budnick, W. A. Hines, and R. Hasegawa, J. Appl. Phys. **55**, 2286 (1984).
[24]K. Raj, A. Amamou, J. Durand, J. I. Budnick, and R. Hasegawa, *Amorphous Magnetism II,* edited by R. A. Levy and R. Hasegawa (Plenum, New York, 1977), p. 221.
[25]Y. Zhang, J. I. Budnick, F. H. Sánchez, W. Hines, Yang, and Livingston, J. Appl. Phys. **61**, 4358 (1987).
[26]R. Hasegawa and R. Ray, J. Appl. Phys. **49**, 4174 (1978).
[27]A. Brown, J. D. Garnish, adn R. W. Honeycombe, Met. Sci. **8**, 317 (1974).
[28]M. T. Clavaguera-Mora, M. D. Baro, S. Surinach, and N. Clavaguera, J. Phys. (Paris) Colloq. (supplement) **51**, C4-49 (1990).
[29]See, for instance, J. Phys. (Paris) Colloq. (supplement) **51**, C4 (1990).